Piezoelectric constants for ZnO calculated using classical polarizable core–shell potentials

2010 Nanotechnology 21 445707

(http://iopscience.iop.org/0957-4484/21/44/445707)

Nanotechnology **21** (2010) 445707 (8pp) doi:10.1088/0957-4484/21/44/445707

Piezoelectric constants for ZnO calculated using classical polarizable core–shell potentials

Shuangxing Dai, Martin L Dunn and Harold S Park

Department of Mechanical Engineering, University of Colorado, Boulder, CO 80309, USA

E-mail: parkhs@bu.edu

Received 16 July 2010, in final form 20 September 2010
Published 8 October 2010
Online at stacks.iop.org/Nano/21/445707

Abstract

We demonstrate the feasibility of using classical atomistic simulations, i.e. molecular dynamics and molecular statics, to study the piezoelectric properties of ZnO using core–shell interatomic potentials. We accomplish this by reporting the piezoelectric constants for ZnO as calculated using two different classical interatomic core–shell potentials: that originally proposed by Binks and Grimes (1994 *Solid State Commun.* **89** 921–4), and that proposed by Nyberg *et al* (1996 *J. Phys. Chem.* **100** 9054–63). We demonstrate that the classical core–shell potentials are able to qualitatively reproduce the piezoelectric constants as compared to benchmark *ab initio* calculations. We further demonstrate that while the presence of the shell is required to capture the electron polarization effects that control the clamped ion part of the piezoelectric constant, the major shortcoming of the classical potentials is a significant underprediction of the clamped ion term as compared to previous *ab initio* results. However, the present results suggest that overall, these classical core–shell potentials are sufficiently accurate to be utilized for large scale atomistic simulations of the piezoelectric response of ZnO nanostructures.

(Some figures in this article are in colour only in the electronic version)

1. Introduction

Bulk piezoelectric materials have long been of interest to scientists and engineers due to their ability to convert mechanical strain into harvestable electrical energy [3, 4], where piezoelectricity is known to occur in materials with non-centrosymmetric crystal structures. However, there has recently been a significant rise in interest and excitement about the potential of piezoelectric nanomaterials; this excitement has taken hold for two key reasons.

First, Wang and co-workers [5–7] recently demonstrated a technique by which an atomic force microscope (AFM) could be utilized to harvest electrical energy from bent ZnO nanowires. Similar findings were reported by other research groups for GaN nanowires [8] and ZnO nanowires [9], though other groups [10] were unable to reproduce the experiments of Wang *et al*.

Second, both experiments [11] and theory [12–14] have demonstrated that due to nanoscale surface effects, ZnO nanostructures have larger piezoelectric constants than are found in bulk ZnO. The larger piezoelectric constants in conjunction with the experimental finding that ZnO nanowires show an increase in their Young's modulus with decreasing nanostructure size [15, 16] are important as they collectively suggest that ZnO nanowires are capable of producing, in relative terms, more mechanical strain energy that can be converted through the piezoelectric effect into harvestable electrical energy than can bulk ZnO [5].

On the theoretical front, researchers have, for about the past 15 years, successfully utilized computational techniques to calculate the piezoelectric constants for piezoelectric materials. In particular, since the development of the Berry phase approach in the early 1990s [17–19], there has been extensive work in using various *ab initio* calculation techniques, and in particular density functional theory (DFT), to calculate the bulk piezoelectric constants for various materials. Examples of such work that specifically address the piezoelectric constants for ZnO include that of Dal Corso *et al* [20], Bernardini *et al* [21], Hill and Waghmare [22], Noel *et al* [23, 24], and Catti *et al* [25].

Table 1. Buckingham and core–shell parameters for the Binks *et al* [1] and Nyberg *et al* [2] core–shell potentials for ZnO.

	Species	A (eV)	ρ (Å)	C (eV Å^6)
Binks	O^{2-}–O^{2-}	9 547.96	0.219 16	32.0
	Zn^{2+}–O^{2-}	529.70	0.358 1	0.0
	Zn^{2+}–Zn^{2+}	0.0	0.0	0.0
Nyberg	O^{2-}–O^{2-}	22 764.0	0.149 0	27.88
	Zn^{2+}–O^{2-}	499.6	0.359 5	0.0
	Zn^{2+}–Zn^{2+}	0.0	0.0	0.0
	Y_+	k_+ (eV Å^{-2})	Y_-	k_- (eV Å^{-2})
Binks	2.00		−2.04	6.3
Nyberg	2.05	8.77	−2.00	15.52

The limitations of *ab initio* approaches to elucidate the size-dependent effects on the piezoelectric properties of nanomaterials are a key motivation for the present work. The major limitation is the fact that *ab initio* calculations, due to computational expense, are typically not utilized to study nanostructures with dimensions larger than about 5 nm. This is problematic when considering recent experimental results [11], which have shown enhancements in the piezoelectric properties of ZnO nanostructures with dimensions exceeding 100 nm. Furthermore, *ab initio* calculations do not account for finite temperature, or thermal effects; this precludes them from elucidating the size-dependent pyroelectric properties of nanostructures.

In contrast, classical atomistic simulations, i.e. molecular dynamics (MD), are inherently able to circumvent some of the length scale and temperature issues associated with *ab initio* calculations. For example, MD simulations are routinely utilized to study nanowires with cross sectional sizes greater than 30 nm [26], and to study nanostructures containing millions of atoms [27]. Furthermore, MD techniques are well developed to study changes in the lattice constants due to variations in both the pressure [28] and the temperature [29]. Therefore, as classical atomistic simulations are well positioned to help bridge the length scale and temperature gap between modeling and experiments to elucidate the size-dependent piezoelectric properties of ZnO nanostructures, it is necessary to develop a fundamental understanding as to the capabilities and shortcomings of classical interatomic potentials in representing the piezoelectric response of ZnO.

However, in contrast to the extensive literature regarding *ab initio* calculations of the piezoelectric constants of ZnO, we have found that there are few such reports on the piezoelectric constants for ZnO calculated using classical interatomic potentials for ZnO, where the interatomic potentials for ZnO are typically based upon the core–shell model originally proposed by Dick and Overhauser [30] in which a massive core is surrounded by a massless, polarizable shell. While these core–shell potentials are limited by the approximation that the charge on the shell remains constant and independent of the state of deformation, it is the polarizable shell that enables these classical potentials to capture polarization in ZnO and other ionic materials.

Table 2. Optimized lattice constants for the Binks *et al* [1] and Nyberg *et al* [2] core–shell potentials for ZnO.

Constant	Binks	Nyberg
a (Å)	3.265	3.2303
c (Å)	5.155	5.0767
u	0.3882	0.389

While classical potentials have not been utilized to study the piezoelectric properties of ZnO, they have recently been utilized to study the electromechanical properties of other materials. For example, Zhang *et al* recently utilized classical core–shell potentials to calculate the size-dependent polarization [31, 32] in $BaTiO_3$ nanowires, while Sharma *et al* have used polarizable charge-based force fields to calculate the size-dependent piezoelectric constants for $BaTiO_3$ nanowires [33]; Sharma *et al* [34] have also utilized core–shell potentials to calculate the flexoelectric constants for various crystalline dielectrics [34], though not ZnO.

It is therefore the objective of the present work to report the piezoelectric constants for ZnO as calculated using two different classical interatomic core–shell potentials, that originally proposed by Binks *et al* [1], and that proposed by Nyberg *et al* [2]. Importantly, the piezoelectric constants were calculated using the same methodology as has been employed in the numerous *ab initio* calculations of piezoelectric constants [20–25]. We demonstrate that the classical potentials are able to qualitatively reproduce the piezoelectric constants as compared to benchmark *ab initio* calculations. We further demonstrate that the presence of the shell is required to capture the electron polarization that controls the clamped ion portion of the piezoelectric constant. The present results suggest that these classical core–shell potentials are sufficiently accurate as to be utilized for large scale atomistic simulations of the piezoelectric response of ZnO nanostructures.

2. Method

The core–shell potentials for ZnO that we consider in the present work take a Buckingham-type form

$$U(r_{ij}) = \frac{q_i q_j}{r_{ij}} + A \exp\left(\frac{-r_{ij}}{\rho}\right) - \frac{C}{r_{ij}^6}, \qquad (1)$$

where the first term on the right-hand side of equation (1) is the long-ranged Coulombic energy, while the second and third terms represent the short-range repulsion and attraction, respectively. We consider two classical core–shell potentials, that of Binks *et al* [1], and that of Nyberg *et al* [2]; we note that the Nyberg *et al* potential is based upon the original potential of Lewis and Catlow [35]. The potential parameters for both potentials are shown in table 1 while the optimum lattice constants for both potentials are shown in table 2; we note that the optimum lattice constants for the Binks potential were found in the work of Hu *et al* [36].

We also note that both the Binks and Nyberg potentials can be represented as either a traditional core-only (rigid ion) potential, or a core–shell potential, in which each point ion

consists of a core of charge X and a shell of charge Y such that the sum of the core and shell charges $(X + Y)$ equals the formal charge of the ion [37, 38]. The key idea behind introducing the additional shell degree of freedom is to enable the ion to polarize in response to an electric field due to the surrounding ions. Note that there is no electrostatic interaction between the core and shell of the same ion, and that the shell model reproduces the ion polarizability α, i.e.

$$\alpha = \frac{Y^2}{K}, \tag{2}$$

where Y is the charge on the shell, which is harmonically coupled to the core through the spring constant K; these core–shell parameters are shown in table 1 for both the Binks and Nyberg potentials.

Both the Binks and Nyberg potentials have been utilized extensively in studies of the mechanical or elastic properties of ZnO nanostructures. For example, the Binks potential was utilized by Kulkarni *et al* [39, 40] to study novel phase transformations in ZnO nanowires; a similar phase transformation was later found using DFT calculations by Alahmed and Fu [41]. The Binks potential was similarly utilized by Agrawal *et al* [16] and Hu *et al* [36, 42] to study the elastic properties of ZnO nanowires, while the properties of the Nyberg potential in capturing the relaxation and structure of ZnO surfaces was extensively studied by Nyberg *et al* [2]. We note that the studies using the Binks potential predicted an increase in the effective nanowire Young's modulus with decreasing nanowire diameter, which is in agreement with recent experiments on ZnO nanowires [15, 16]. However, it is critical to note that in the majority of these simulations, particularly those involving the Binks potential [16, 36, 39, 40, 42], the effects of the core–shell interactions were not considered.

3. Piezoelectric constants

In previous *ab initio* work [20–25], the piezoelectric constants e_{33}, e_{31}, and e_{15}, were calculated according to the following relationship [25]:

$$e_{ij} = e_{ij}^{(0)} + e_{ij}^{\text{int}}, \tag{3}$$

$$e_{ij}^{(0)} = \left.\frac{\partial P_i}{\partial \epsilon_j}\right|_u, \tag{4}$$

$$e_{ij}^{\text{int}} = \left.\frac{\partial P_i}{\partial u}\right|_{\epsilon_j} \frac{\mathrm{d}u}{\mathrm{d}\epsilon_j}. \tag{5}$$

In equations (3)–(5), $e_{ij}^{(0)}$ is the clamped ion term, which in *ab initio* calculations represents the influence of electron delocalization on the piezoelectric properties, while e_{ij}^{int} is called the internal strain term, and represents the contribution of the change in atomic fractional coordinates u to the piezoelectric properties [25].

To calculate the piezoelectric constants using the classical core–shell potentials described in the present work, we first define the polarization P_3 as

$$P_3 = P_3\left(u(\epsilon_3), \epsilon_3\right) = P_3^{\text{elec}}(\epsilon_3) + P_3^{\text{dis}}\left(u(\epsilon_3)\right), \tag{6}$$

from which the piezoelectric constants, for example e_{33}, can be calculated as

$$\begin{aligned} e_{33} &= \frac{\partial P_3}{\partial \epsilon_3} = \frac{\partial P_3^{\text{elec}}(\epsilon_3)}{\partial \epsilon_3} + \frac{\partial P_3^{\text{dis}}\left(u(\epsilon_3)\right)}{\partial \epsilon_3}, \\ &= \frac{\partial P_3^{\text{elec}}(\epsilon_3)}{\partial \epsilon_3} + \frac{\partial P_3^{\text{dis}}\left(u(\epsilon_3)\right)}{\partial u(\epsilon_3)} \frac{\mathrm{d}u(\epsilon_3)}{\mathrm{d}\epsilon_3}, \\ &= \left.\frac{\partial P_3}{\partial \epsilon_3}\right|_u + \left.\frac{\partial P_3}{\partial u(\epsilon_3)}\right|_{\epsilon_3} \frac{\mathrm{d}u(\epsilon_3)}{\mathrm{d}\epsilon_3}, \\ &= e_{33}^{(0)} + e_{33}^{\text{int}}, \end{aligned} \tag{7}$$

where $P_3^{\text{dis}}(u(\epsilon_3))$ represents the displacement-based polarization due to changes in the fractional atomic coordinate u, i.e. due to the relative displacement between the zinc and oxygen atoms, P_3^{elec} is the polarization that occurs due to the relative separation between the core and the shell, and where in our molecular statics calculations, the polarization P_3 is calculated as:

$$\begin{aligned} P_3 &= e_{31}\epsilon_1 + e_{32}\epsilon_2 + e_{33}\epsilon_3, \\ &= \frac{\sum_i \vec{r}_i q_i}{V_{\text{cell}}} = \frac{-4qu}{\sqrt{3}a_0^2(1+\epsilon_1)(1+\epsilon_2)}, \end{aligned} \tag{8}$$

where $e_{31} = e_{32}$, $\epsilon_1 = \epsilon_2 = \epsilon = (a - a_0)/a_0$, $\epsilon_3 = (c - c_0)/c_0$.

The classical decomposition in equations (6) and (7) was chosen such that a direct correlation between the terms in the *ab initio* decomposition in equation (3) and the classical decomposition could be made. First, it can be seen that the second term on the right-hand side of equation (7) directly corresponds to the internal strain terms in the *ab initio* expression in equation (3). Second, we can clearly see that the classical analog to the electron delocalization effect, which is the basis for the clamped ion term $e_{33}^{(0)}$ in equation (3), is the electron polarization which arises entirely from the relative separation between the core and shell. Furthermore, it can be seen in equation (7) that if the shell is not considered in the classical theory, i.e. the rigid ion approximation is used, then the clamped ion term $e_{33}^{(0)} = 0$ as there can be no polarization between the core and the shell [25].

We also note that the approach delineated in equations (3)–(7) does not work for all polarizable core–shell potentials. For example, we consider the core–shell potential for GaN developed by Zapol *et al* [38]. In that potential, the effective charges on the Ga and N ions are taken to be $\pm 2e$, to account for the partially covalent and partially ionic nature of the bonding. However, the actual effective charges as calculated by *ab initio* calculations are about $\pm 2.7e$ [21]. The problem with this charge reduction is that it results in a polarization P_3 that is about 33% smaller than it should be as compared to an *ab initio* calculation simply because the value of the polarization depends on the effective charge q, as seen in equation (8). This issue does not arise for ZnO because the effective charges as calculated using *ab initio* are about $\pm 2.05e$ [20], which are nearly identical to the classical values seen in table 1. Therefore, the *ab initio* methodology of calculating the piezoelectric constants described in equations (3)–(7) will not work for the particular potential of Zapol *et al* [38] without a modification to the effective charges of the Ga and N ions.

To calculate these piezoelectric constants using classical atomistic simulations, it is important to distinguish between

Table 3. Summary of piezoelectric constants e_{33} calculated using classical interatomic potentials, both with and without the shell, as compared with the DFT results summarized in tables 2 and 5 of Noel *et al* [23]; P_{eq} is the spontaneous polarization, in units of C m^{-2}.

Method	No shell	No shell	Shell	Shell	DFT
Potential	Binks	Nyberg	Binks	Nyberg	
P_{eq}	−0.092	−0.099	−0.092	−0.099	−0.029 → −0.057
$du/d\epsilon_3$	−0.182	−0.182	−0.217	−0.211	−0.21 → −0.254
$\partial P_3/\partial u$	−6.94	−7.09	−6.94	−7.09	−7.10 → −7.60
$e_{33}^{(0)}$	0	0	−0.26	−0.22	−0.45 → −0.73
$e_{33}^{(0)}/e_{33}^{int}$	0	0	−0.173	−0.147	−0.272 → −0.353
$\tilde{e}_{33} = e_{33}$	1.27	1.29	1.25	1.27	0.89 → 1.31

the proper and improper piezoelectric constants [25, 43]. As noted by Vanderbilt [43], the improper piezoelectric tensor is calculated as

$$e_{ijk} = \frac{\partial P_i}{\partial \epsilon_{jk}}, \tag{9}$$

where we note that throughout this work, we have used Voigt's notation for the piezoelectric constants. The issue with the improper piezoelectric constants is that they do not account for the fact that the polarization is a multi-valued function that depends upon the position in the crystal lattice where it is evaluated; this point is articulated in detail by Vanderbilt [43]. Therefore, in order to calculate proper, or invariant piezoelectric constants, we utilized the expression [43]

$$\tilde{e}_{ijk} = e_{ijk} + \delta_{jk} P_i - \delta_{ij} P_k. \tag{10}$$

The three proper piezoelectric constants that we will calculate in the present work are defined as:

$$\tilde{e}_{33} = e_{33}, \qquad \tilde{e}_{31} = e_{31} + P_3, \qquad \tilde{e}_{15} = e_{15} - P_3. \tag{11}$$

where the clamped ion term should also be calculated using the proper definition [44]:

$$\tilde{e}_{ijk}^{(0)} = e_{ijk}^{(0)} + \delta_{jk} P_i^{\text{elec}} - \delta_{ij} P_k^{\text{elec}}. \tag{12}$$

The piezoelectric constants were calculated by considering a wurtzite ZnO nanostructure with 10 × 10 × 10 unit cells in each dimension for a total of 4000 atoms; periodic boundary conditions were imposed in all three coordinate directions to mimic a bulk ZnO crystal. The size of the periodic nanostructure was slightly different between the Binks and Nyberg potentials owing to the different lattice constants a and c seen in table 2; the sizes were 3.265 nm × 2.828 nm × 5.155 nm for the Binks potential and 3.230 nm × 2.798 nm × 5.077 nm for the Nyberg potential. All classical atomistic simulations were performed using the general purpose molecular simulation code Gromacs [45], where the long-range Coulombic forces and energies were calculated using the Ewald summation technique.

Small strains between −1 and 1% were applied using the strain states defined below to calculate the piezoelectric constants. Specifically, the strain applied to calculate e_{33} was prescribed as, following Catti *et al* [25], [0 0 ε 0 0 0], giving:

$$\tilde{e}_{33} = \frac{\partial P_3}{\partial \epsilon_3} = e_{33} = \frac{-4q}{\sqrt{3}a_0^2}\frac{du}{d\epsilon_3}. \tag{13}$$

For e_{31}, the applied strain was [ε ε 0 0 0 0], giving:

$$\tilde{e}_{31} = \frac{\partial P_3}{\partial \epsilon_1} + P_3 = e_{31} + P_3 = \frac{a_0}{2}\frac{\partial P_3}{\partial a} + P_3 = \frac{-2q}{\sqrt{3}a_0^2}\frac{du}{d\varepsilon}. \tag{14}$$

For e_{15}, the strain was [0 0 0 2ε 2$\sqrt{3}\varepsilon$ 0], giving:

$$\tilde{e}_{15} = e_{15} - P_3 = \frac{\partial P_1}{\partial \epsilon_5} - P_3 = \frac{1}{2\sqrt{3}}\frac{dP_1}{d\epsilon} - P_3. \tag{15}$$

We emphasize that the expressions on the right-hand sides of equations (13)–(15) correspond to the values that can be obtained analytically for a classical rigid ion model (i.e. neglecting the effects of the shell) as described by Catti *et al* [25], which corresponds to considering the displacement polarization only in equation (6). In particular, because the classical rigid ion model cannot capture electron polarization due to the relative core–shell displacements, the factor multiplying the $du/d\epsilon$ term on the right-hand sides of equations (13) and (14) corresponds to the $\partial P_3/\partial u$ part of the piezoelectric constant in equation (7).

4. Numerical results

The results for the piezoelectric constant $\tilde{e}_{33}$ calculated using the two classical potentials are summarized in table 3. There, all terms, including the clamped ion term $e_{33}^{(0)}$, and the two terms comprising the internal strain term, along with the proper and improper piezoelectric constants are tabulated and compared to the range of DFT values given in tables 2 and 5 of Noel *et al* [23]. The plots resulting from the atomistic simulations from which the values in table 3 were generated are shown in figure 1; we note that the values in table 3 were obtained by performing linear fits to the data in figure 1. We note that the no shell values in table 3, which correspond to evaluating only the displacement polarization P_3^{dis} in equation (6), can also be obtained directly by evaluating equation (13).

The first thing we observe is that, regardless of whether the shell is utilized or ignored, the piezoelectric constant $e_{33} = \tilde{e}_{33}$ for both potentials falls within the range of previously published DFT values [23]. We note that the term $\partial P_3/\partial u$ can be calculated analytically as shown in equation (13) from the expression

$$\left.\frac{\partial P_3}{\partial u}\right|_{\epsilon_3} = -\frac{4q}{\sqrt{3}a_0^2}. \tag{16}$$

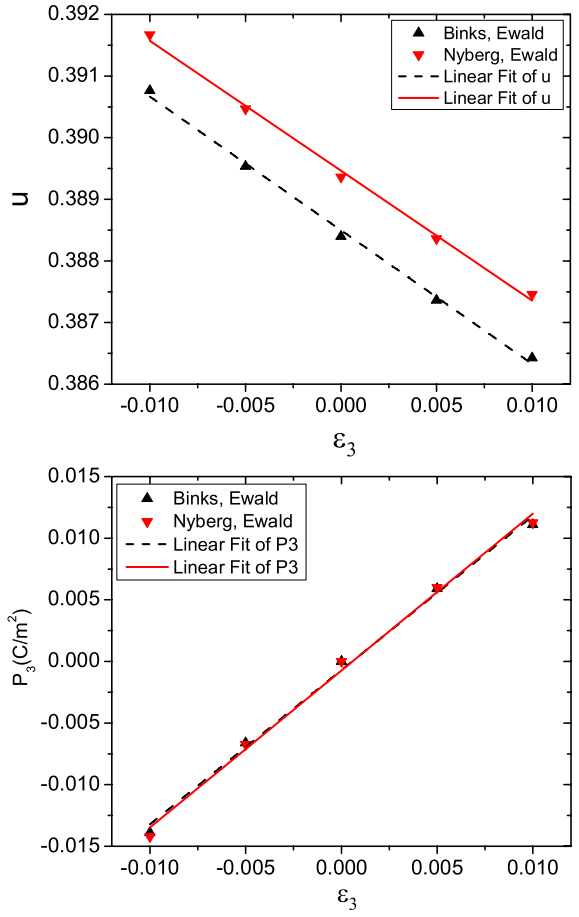

Figure 1. Plots utilized to calculate the piezoelectric constant e_{33}. Top: equilibrium fractional coordinate u as a function of the strain ϵ_3. Bottom: polarization P_3 as a function of the strain ϵ_3.

It is clear from equation (16) that $\partial P_3/\partial u$ depends only upon the lattice constant a_0, which is potential dependent; this explains why the Binks and Nyberg potentials in table 3 have slightly different values for this term.

We also list values for the spontaneous polarization $P_{\rm eq}$ in table 3, where $P_{\rm eq}$ is defined as the difference in polarization P_3 between the ideal wurtzite crystal state (i.e. when $u = 0.375$), and the minimum energy configuration for the ZnO crystal, which occurs at values of $u = 0.3882$ and 0.389 for the two potentials we have considered. This difference in lattice constants also explains why the spontaneous polarization $P_{\rm eq}$ that is calculated using the Binks (-0.092) and Nyberg (-0.099) potentials is about a factor of two to three times larger than the values ranging from about -0.03 to -0.06 that have been reported using DFT calculations [23]. Specifically, because the minimum energy configurations for both potentials occur for the lattice ratio $u = 0.3882$ or $u = 0.389$ in table 2, both of which are larger than the value of $u = 0.382$ that was reported in the previous DFT calculations [23], the spontaneous polarization that is predicted by the classical potentials is correspondingly larger.

However, if the individual terms comprising the piezoelectric constant, i.e. the clamped ion and internal strain terms, are considered, the importance of considering the shell becomes apparent. First, table 3 demonstrates that when the shell is considered, for both the Nyberg and Binks potentials, the $\mathrm{d}u/\mathrm{d}\epsilon_3$ term becomes more negative due to increased relaxation effects, and thus becomes more accurate as compared to the DFT results which range between -0.21 and -0.254. More importantly, table 3 demonstrates that when the shell is neglected, the clamped ion term $e_{33}^{(0)} = 0$, which is obviously incorrect physically. This result is consistent with the result given by Catti *et al* [25], who noted that any rigid ion model will give a zero clamped ion term for a periodic system.

However, when the core–shell interactions are accounted for, the clamped ion term $e_{33}^{(0)}$ for the Binks and Nyberg potentials take values of -0.26 and -0.22, respectively. While these values have the correct sign, they are about 50% smaller than the lower bound DFT value of -0.45. Furthermore, the underprediction of the clamped ion term has a strong effect on the expected ratio between the clamped ion and internal strain contributions to the piezoelectric constant ($e_{33}^{(0)}/e_{33}^{\rm int}$) seen in table 3. Specifically, that ratio as calculated using both classical core–shell potentials is also at least 50% smaller than the expected ratio from previous DFT calculations. Both of these results are likely due to the fact that while the core–shell spring constant in equation (2) was fit to reproduce the ion polarizability [1, 2, 35], it was not fit to reproduce the piezoelectric constants, i.e. a softer spring connecting the core and the shell would lead to a larger electron polarization.

Overall, the classical potentials qualitatively capture the tendency found in DFT calculations of the piezoelectric constants of ZnO that the clamped ion contribution $e_{33}^{(0)}$ to the total piezoelectric constant $\tilde{e}_{33}$ is relatively small as compared to other tetrahedrally bonded semiconductors such as ZnS [20], which indicates that the core–shell potentials capture the importance of strain-induced internal relaxation between anion and cation sublattices for the piezoelectric response of ZnO.

The results for the piezoelectric constant $\tilde{e}_{31}$ calculated using the two classical potentials are summarized in table 4. There, all terms, including the clamped ion term $e_{31}^{(0)}$, and the two terms comprising the internal strain term, along with the proper and improper piezoelectric constants are tabulated and compared to the range of DFT values given in table 5 of Noel *et al* [23]. We also show in table 4 the value of the polarization P_3 that is needed to evaluate the proper piezoelectric constant $\tilde{e}_{31}$ in equation (14), where P_3 is the value of the polarization that is calculated assuming the equilibrium, zero strain lattice constants for each potential that are given in table 2.

The plots resulting from the atomistic simulations from which the values in table 4 were generated are shown in figure 2. We note that the biaxial nature of the strain that is needed to calculate e_{31} is written as

$$\frac{\mathrm{d}u}{\mathrm{d}\epsilon_{12}} = \frac{\mathrm{d}u}{\mathrm{d}(\epsilon_1 + \epsilon_2)} = \frac{1}{2}\frac{\mathrm{d}u}{\mathrm{d}\epsilon}, \tag{17}$$

while

$$e_{31} = \frac{\partial P_3}{\partial \epsilon_1} = \frac{1}{2}\frac{\partial P_3}{\partial \epsilon}. \tag{18}$$

As can be seen in table 4, the terms comprising the piezoelectric constant e_{31} that were calculated using the classical potentials again show reasonable agreement with those obtained from DFT, with similar trends and shortcomings

Table 4. Summary of the proper ($\tilde{e}_{31}$) and improper (e_{31}) piezoelectric constants calculated using classical interatomic potentials, both with and without the shell, as compared with the DFT results summarized in table 5 of Noel *et al* [23].

Method	No shell	No shell	Shell	Shell	DFT
Potential	Binks	Nyberg	Binks	Nyberg	
$du/d\epsilon$	0.078	0.069	0.095	0.084	$0.108 \rightarrow 0.131$
$\partial P_3/\partial u$	−6.94	−7.09	−6.94	−7.09	$-7.10 \rightarrow -7.60$
P_3	−2.695	−2.759	−2.695	−2.759	
$e_{31}^{(0)}$	0	0	0.13	0.11	$0.22 \rightarrow 0.38$
$e_{31}^{(0)}/e_{31}^{\text{int}}$	0	0	0.199	0.185	$0.287 \rightarrow 0.343$
$\tilde{e}_{31}$	−0.54	−0.49	−0.53	−0.48	$-0.51 \rightarrow -0.69$
e_{31}	2.15	2.27	2.16	2.28	

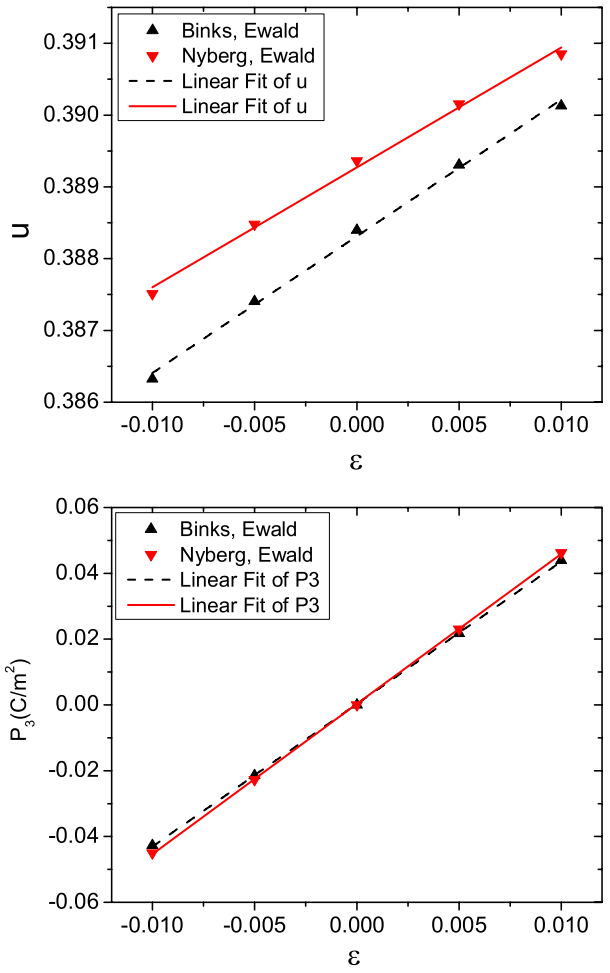

Figure 2. Plots utilized to calculate the piezoelectric constant e_{31}. Top: equilibrium fractional coordinate u as a function of the biaxial strain ϵ. Bottom: polarization P_3 as a function of the biaxial strain ϵ.

as observed previously in table 3 for e_{33}. Specifically, the value for $du/d\epsilon$, while positive for e_{31} rather than negative, increases and becomes more accurate as compared to the DFT results when the shell is included. Similarly, the clamped ion term $e_{31}^{(0)}$ is zero when the shell is ignored, but takes on a finite, positive value when the shell is considered.

We also note that due to the opposite signs that are observed for $du/d\epsilon$ and $\partial P_3/\partial u$ in table 4, the internal strain term e_{31}^{int} is negative. This is important as it means that the classical core–shell potentials are able to capture, in a qualitative manner, the fact that the biaxial strain state described in equation (17) produces inner ionic relaxations that oppose the strain directions, as is expected from previous DFT calculations [25].

Table 5. Summary of the proper ($\tilde{e}_{15}$) and improper (e_{15}) piezoelectric constants calculated using classical interatomic potentials, both with and without the shell, compared with the DFT results summarized in table 3 of Catti *et al* [25].

Method	No shell	No shell	Shell	Shell	DFT
Potential	Binks	Nyberg	Binks	Nyberg	
$dP_1/d\epsilon$	−11.013	−11.162	−11.003	−11.150	
P_3	−2.693	−2.752	−2.693	−2.752	
$e_{15}^{(0)}$	0	0	0.0426	0.0413	0.22
$\tilde{e}_{15}$	−0.486	−0.470	−0.483	−0.466	−0.46
e_{15}	−3.179	−3.222	−3.176	−3.219	

Similar to the clamped ion term $e_{33}^{(0)}$, the value of the clamped ion term $e_{31}^{(0)}$ is at least 50% smaller than the corresponding DFT value. This underprediction of the clamped ion term also manifests itself in the ratio between the clamped ion and internal strain contributions to the piezoelectric constant $\tilde{e}_{31}$ in table 4. Specifically, the $e_{31}^{(0)}/e_{31}^{\text{int}}$ ratio as calculated using the classical core–shell potentials is again about 40–50% smaller than the expected ratios from previous DFT calculations.

Table 4 also demonstrates the necessity of calculating the proper piezoelectric constant $\tilde{e}_{31}$ using equation (10) rather than the improper piezoelectric constant e_{31}. Specifically, the improper piezoelectric constant e_{31} takes on a large, positive value. However, when the polarization P_3 is added back to e_{31}, small negative values of $\tilde{e}_{31}$ are obtained that are in line with previous DFT calculations.

Lastly we discuss the final piezoelectric constant of interest e_{15}; the calculated values using both core–shell potentials is shown in table 5, while the plot of the polarization versus the strain from which the piezoelectric constants were obtained is shown in figure 3. We note first that following from equation (11), the proper ($\tilde{e}_{15}$) and improper (e_{15}) values of the piezoelectric constant should be different, as is observed in table 5. Second, we note that the polarization P_1 vanishes for ZnO at zero strain; this is due to the symmetry of the wurtzite crystal that exists in the plane of the crystal.

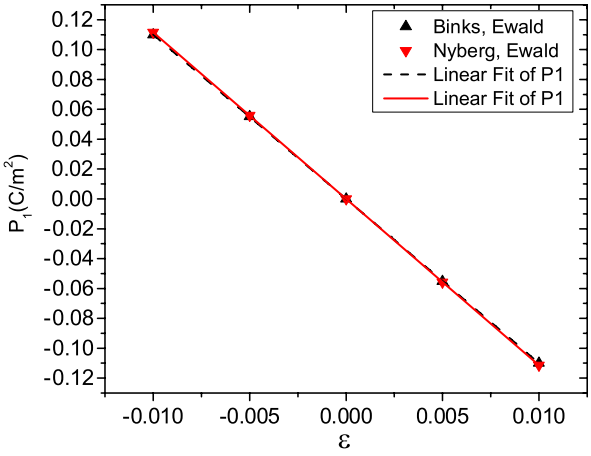

Figure 3. Polarization P_1 versus strain ϵ plot that was utilized to calculate the piezoelectric constant e_{15}.

The trends are similar as for the previously calculated piezoelectric constants $\tilde{e}_{33}$ and $\tilde{e}_{31}$. Specifically, the clamped ion term in this case is significantly smaller, by nearly an order of magnitude, as compared to the DFT calculation; however, it does have the correct sign. However, similar to what was found for the other piezoelectric constants $\tilde{e}_{33}$ and $\tilde{e}_{31}$, the calculated value for $\tilde{e}_{15}$ is found to be comparable to the reported DFT value.

One possible reason for the very small value of the clamped ion term for e_{15} arises due to the isotropic nature of the spring force that describes the core–shell interactions [1, 2, 35]. Specifically, because the shear strains that are needed to calculate e_{15} result in smaller changes in bond lengths than either the uniaxial or biaxial tension that is applied to calculate e_{33} or e_{31}, a smaller force is generated to separate the core and shell in shear, thus leading to a smaller electron polarization. It therefore seems possible that e_{15} could be improved by utilizing an anisotropic spring force between the core and the shell, for example as described by van Maaren and Spoel [46].

5. Conclusions

We have demonstrated that classical polarizable core–shell interatomic potentials are able to qualitatively capture the piezoelectric properties of bulk ZnO as compared to benchmark DFT calculations. Specifically, we have demonstrated that when the effects of the polarizable shell are accounted for, the core–shell potentials are able to qualitatively capture the effects of the clamped ion contribution to the piezoelectric constants.

The main shortcoming of the classical potentials is that they significantly underpredict the value of the clamped ion contribution $e_{ij}^{(0)}$ to each of the piezoelectric constants, though it may be possible to improve this by directly fitting the core–shell parameters to reproduce the piezoelectric constants for the material of interest. Despite this shortcoming, the present results suggest that classical polarizable core–shell interatomic potentials should be sufficiently accurate to be useful in analyzing the piezoelectric properties of ZnO nanostructures via large scale atomistic simulations.

Acknowledgments

HSP and SD gratefully acknowledge the support of the NSF, grant CMMI-0856261. HSP and SD also acknowledge helpful discussions with J Hu, R Agrawal and P Sharma. MLD acknowledges support by the DARPA Center on Nanoscale Science and Technology for Integrated Micro/Nano-Electromechanical Transducers (iMINT) funded by the DARPA N/MEMS S&T Fundamentals Program (HR0011-06-1-0048).

References

[1] Binks D J and Grimes R W 1994 The non-stoichiometry of zinc and chromium excess zinc chromite *Solid State Commun.* **89** 921–4
[2] Nyberg M, Nygren M A, Pettersson L G M, Gay D H and Rohl A L 1996 Hydrogen dissociation on reconstructed ZnO surfaces *J. Phys. Chem.* **100** 9054–63
[3] Roundy S 2005 On the effectiveness of vibration-based energy harvesting *J. Intell. Mater. Syst. Struct.* **16** 809–23
[4] Anton S R and Sodano H A 2007 A review of power harvesting using piezoelectric materials (2003–2006) *Smart Mater. Struct.* **16** R1–21
[5] Wang Z L and Song J 2006 Piezoelectric nanogenerators based on zinc oxide nanowire arrays *Science* **312** 242–6
[6] Gao P X, Song J, Liu J and Wang Z L 2007 Nanowire piezoelectric nanogenerators on plastic substrates as flexible power sources for nanodevices *Adv. Mater.* **19** 67–72
[7] Song J, Zhou J and Wang Z L 2006 Piezoelectric and semiconducting coupled power generating process of a single ZnO belt/wire. a technology for harvesting electricity from the environment *Nano Lett.* **6** 1656–62
[8] Su W S, Chen Y F, Hsiao C L and Tu L W 2007 Generation of electricity in GaN nanorods induced by the piezoelectric effect *Appl. Phys. Lett.* **90** 063110
[9] Scrymgeour D A and Hsu J W P 2008 Correlated piezoelectric and electrical properties in individual ZnO nanorods *Nano Lett.* **8** 2204–9
[10] Alexe M, Senz S, Schubert M A, Hesse D and Gosele U 2008 Energy harvesting using nanowires? *Adv. Mater.* **20** 4021–6
[11] Zhao M-H, Wang Z-L and Mao S X 2004 Piezoelectric characterization of individual zinc oxide nanobelt probed by piezoresponse force microscope *Nano Lett.* **4** 587–90
[12] Xiang H J, Yang J, Hou J G and Zhu Q 2006 Piezoelectricity in ZnO nanowires: a first-principles study *Appl. Phys. Lett.* **89** 223111
[13] Li C, Guo W, Kong Y and Gao H 2007 Size-dependent piezoelectricity in zinc oxide nanofilms from first-principles calculations *Appl. Phys. Lett.* **90** 033108
[14] Mitrushchenkov A, Linguerri R and Chambaud G 2009 Piezoelectric properties of AlN, ZnO, and $Hg_xZn_{1-x}O$ nanowires by first-principles calculations *J. Phys. Chem.* C **113** 6883–6
[15] Chen C Q, Shi Y, Zhang Y S, Zhu J and Yan Y J 2006 Size dependence of the young's modulus of ZnO nanowires *Phys. Rev. Lett.* **96** 075505
[16] Agrawal R, Peng B, Gdoutos E and Espinosa H D 2008 Elasticity size effects in ZnO nanowires—a combined experimental-computational approach *Nano Lett.* **8** 3668–74
[17] King-Smith R D and Vanderbilt D 1993 Theory of polarization of crystalline solids *Phys. Rev.* B **47** 1651–4
[18] Resta R 1994 Macroscopic polarization in crystalline dielectrics: the geometric phase approach *Rev. Mod. Phys.* **66** 899–915

[19] Vanderbilt D and King-Smith R D 1993 Electric polarization as a bulk quantity and its relation to surface charge *Phys. Rev.* B **48** 4442–55
[20] Dal Corso A, Posternak M, Resta R and Baldereschi A 1994 *Ab initio* study of piezoelectricity and spontaneous polarization in ZnO *Phys. Rev.* B **50** 10715–21
[21] Bernardini F, Fiorentini V and Vanderbilt D 1997 Spontaneous polarization and piezoelectric constants of III–V nitrides *Phys. Rev.* B **56** 10024–7
[22] Hill N A and Waghmare U 2000 First-principles study of strain-electronic interplay in ZnO: stress and temperature dependence of the piezoelectric constants *Phys. Rev.* B **62** 8802–10
[23] Noel Y, Llunell M, Orlando R, D'Arco P and Dovesi R 2002 Performance of various hamiltonians in the study of the piezoelectric properties of crystalline compounds: the case of BeO and ZnO *Phys. Rev.* B **66** 214107
[24] Noel Y, Zicovich-Wilson C M, Civalleri B, D'Arco P and Dovesi R 2002 Polarization properties of ZnO and BeO: an *ab initio* study through the berry phase and wannier functions approaches *Phys. Rev.* B **65** 014111
[25] Catti M, Noel Y and Dovesi R 2003 Full piezoelectric tensors of wurtzite and zinc blende ZnO and ZnS by first-principles calculations *J. Phys. Chem. Solids* **64** 2183–90
[26] Leach A M, McDowell M and Gall K 2007 Deformation of top-down and bottom-up silver nanowires *Adv. Funct. Mater.* **17** 43–53
[27] Vashishta P, Kalia R K and Nakano A 2003 Multimillion atom molecular dynamics simulations of nanostructures on parallel computers *J. Nanoparticle Res.* **5** 119–35
[28] Berendsen H J C, Postma J P M, Van Gunsteren W F, DiNola A and Haak J R 1984 Molecular dynamics with coupling to an external bath *J. Chem. Phys.* **81** 3684–90
[29] Hoover W G 1985 Canonical dynamics: equilibrium phase-space distributions *Phys. Rev.* A **31** 1695–7
[30] Dick B G and Overhauser A W 1958 Theory of the dielectric constants of alkali halide crystals *Phys. Rev.* **112** 90–103
[31] Zhang Y, Hong J, Liu B and Fang D 2009 Molecular dynamics investigations on the size-dependent ferroelectric behavior of $BaTiO_3$ nanowires *Nanotechnology* **20** 405703
[32] Zhang Y, Hong J, Liu B and Fang D 2010 Strain effect on ferroelectric behaviors of $BaTiO_3$ nanowires: a molecular dynamics study *Nanotechnology* **21** 015701
[33] Majdoub M S, Sharma P and Cagin T 2008 Enhanced size-dependent piezoelectricity and elasticity in nanostructures due to the flexoelectric effect *Phys. Rev.* B **77** 125424
[34] Maranganti R and Sharma P 2009 Atomistic determination of flexoelectric properties of crystalline dielectrics *Phys. Rev.* B **80** 054109
[35] Lewis G V and Catlow C R A 1985 Potential models for ionic oxides *J. Phys. C: Solid State Phys.* **18** 1149–61
[36] Hu J, Liu X W and Pan B C 2008 A study of the size-dependent elastic properties of ZnO nanowires and nanotubes *Nanotechnology* **19** 285710
[37] Sun X, Chen Q, Chu Y and Wang C 2005 Structural and thermodynamic properties of GaN at high pressures and high temperatures *Physica* B **368** 243–50
[38] Zapol P, Pandey R and Gale J D 1997 An interatomic potential study of the properties of gallium nitride *J. Phys.: Condens. Matter* **9** 9517–25
[39] Kulkarni A J, Zhou M and Ke F J 2005 Orientation and size dependence of the elastic properties of zinc oxide nanobelts *Nanotechnology* **16** 2749–56
[40] Kulkarni A J, Zhou M, Sarasamak K and Limpijumnong S 2006 Novel phase transformation in ZnO nanowires under tensile loading *Phys. Rev. Lett.* **97** 105502
[41] Alahmed Z and Fu H 2008 Polar semiconductor ZnO under inplane tensile strain *Phys. Rev.* B **77** 045213
[42] Hu J and Pan B C 2009 Surface effect on the size- and orientation-dependent elastic properties of single-crystal ZnO nanostructures *J. Appl. Phys.* **105** 034302
[43] Vanderbilt D 2000 Berry-phase theory of proper piezoelectric response *J. Phys. Chem. Solids* **61** 147–51
[44] Saghi-Szabo G, Cohen R E and Krakauer H 1998 First-principles study of piezoelectricity in $PbTiO_3$ *Phys. Rev. Lett.* **80** 4321–4
[45] Hess B, Kutzner C, van der Spoel D and Lindahl E 2008 GROMACS 4: algorithms for highly efficient, load-balanced, and scalable molecular simulation *J. Chem. Theory Comput.* **4** 435–47
[46] van Maaren P J and van der Spoel D 2001 molecular dynamics simulations of water with novel shell-model potentials *J. Phys. Chem.* B **105** 2618–26